

# Phenotypic and genotypic characterisation of *Blastocystis hominis* isolates implicates subtype 3 as a subtype with pathogenic potential

T. C. Tan · K. G. Suresh · H. V. Smith

Received: 31 July 2008 / Accepted: 13 August 2008 / Published online: 16 September 2008  
© Springer-Verlag 2008

**Abstract** Despite frequent reports on the presence of *Blastocystis hominis* in human intestinal tract, its pathogenicity remains a matter of intense debate. These discrepancies may be due to the varying pathogenic potential or virulence of the isolates studied. The present study represents the first to investigate both phenotypic and genotypic characteristics of *B. hominis* obtained from symptomatic and asymptomatic individuals. Symptomatic isolates had a significantly greater size range and lower growth rate in Jones' medium than asymptomatic isolates. The parasite cells of symptomatic isolates exhibited rougher surface topography and greater binding affinity to *Canavalia ensiformis* (ConA) and *Helix pomatia* (HPA). The present study also identifies further phenotypic characteristics, which aided in differentiating the pathogenic forms from the non-pathogenic forms of *B. hominis*. *Blastocystis* subtype 3 was found to be correlated well with the disease.

## Introduction

Despite being discovered more than 90 years ago, the pathogenicity of *Blastocystis hominis* has not been conclusively determined, although it remains one of the most common intestinal protozoan parasites of humans. The possibility that virulent and avirulent isolates of *Blastocystis* exist, or that pathogenicity is due to different species of

*Blastocystis* has been often suggested because *B. hominis* is antigenically and genetically heterogeneous both within and among geographic regions (Tan et al. 2002). In vitro, *Blastocystis* can exhibit diverse morphologies and reproductive processes (Suresh et al. 2003), but whether different life cycle stages influence pathogenicity remains to be elucidated. A review of the literature reveals that certain researchers implicate *B. hominis* as a pathogen while others think otherwise. The discrepancies may, in part, be due to the fact that different researchers studied distinct *Blastocystis* isolates, which had varying pathogenic potential (Clark 1997).

Recent studies investigating the pathogenic potential of *Blastocystis* in humans have focused on genotypic analysis (e.g. Böhm-Gloning et al. 1997; Kaneda et al. 2001; Yoshikawa et al. 2004; Yan et al. 2006; Stensvold et al. 2007a,b) without providing phenotypic information on the isolates studied. Therefore, no comparisons of phenotypic similarities or differences can be made between the isolates that these researchers subtyped. As current genotyping methods cannot discriminate between symptomatic and asymptomatic isolates, an obvious approach would be to investigate the use of both phenotypic and genotypic approaches to determining pathogenicity. Here, we investigate both phenotypic and genotypic perspectives of *B. hominis* isolates obtained from symptomatic and asymptomatic individuals in order to determine whether such an approach can assist in determining pathogenicity.

## Materials and methods

### Source of *Blastocystis hominis* isolates

A total of 20 human-derived *B. hominis* isolates, comprising ten asymptomatic (A1–A10) and ten symptomatic (S1–S10)

T. C. Tan · K. G. Suresh (✉)  
Department of Parasitology, Faculty of Medicine,  
University of Malaya,  
Kuala Lumpur, Malaysia  
e-mail: suresh@um.edu.my

H. V. Smith  
Scottish Parasite Diagnostic Laboratory, Stobhill Hospital,  
Glasgow G21 3UW Scotland, UK

isolates were investigated. Both inclusion criteria and details of the subjects, together with their clinical histories have been described previously (Tan and Suresh 2006a).

#### Culture of *B. hominis* isolates

Parasites were isolated from clinical cases and healthy individuals by in vitro cultivation in Jones' medium (Jones 1946) supplemented with 10% horse serum at 37°C (Suresh et al. 1994; Zaman 1997; Suresh and Smith 2004). A stool sample the size of a pea (500 mg–1 g) was comminuted in 3 ml of Jones' medium. For liquid stools, about 750 µl was mixed with 3 ml of Jones' medium. Subsequently, parasites were maintained in Jones' medium by subculturing every 3 to 4 days for at least 1 month prior to phenotypic analyses.

#### Growth characteristics

Parasites from 3-day-old cultures of each isolate were grown separately at a final concentration of  $1 \times 10^4$  cells per ml in 3 ml of fresh Jones' medium containing 10% horse serum. All experiments were performed in triplicate. Parasites were enumerated daily for up to 10 days using an improved Neubauer hemocytometer chamber (Hausser Scientific) with 0.5% Trypan blue solution as an indicator of viability (Fauque et al. 2007). Only viable cells that excluded Trypan blue were enumerated. The generation time (GT) was calculated for the 24-h period during which the most rapid growth occurred, according to the formula described by Zierdt and Swan (1981). Fifty parasites were randomly selected from each culture for size measurement every 48 h for up to 10 days, after their initial inoculation in Jones' medium and the percentages of vacuolar, granular and amoeboid forms were calculated daily. Statistical analyses were carried out using SPSS version 11.

#### Scanning electron microscopy

Three asymptomatic isolates (A1, A3 and A4) and three symptomatic isolates (S1, S8 and S10) were selected randomly for ultrastructural studies. The contents of the day-5 culture (peak parasite count, see Fig. 1) were washed five times with phosphate-buffered saline (PBS, 150 mM, pH 7.4) and centrifuged ( $500 \times g$ , 5 min). Pelleted cells were fixed in 4% glutaraldehyde then post-fixed in 1% osmium tetroxide. Post-fixed specimens were mounted on polycarbonate membranes (Nucleopore, Agar Scientific, USA) and dehydrated through increasing concentrations (10%, 20%, 30%, 40%, 50%, 60%, 70%, 80%, 90%, 95%, 10 min each) of ethanol, critical-point dried with carbon dioxide, coated with gold, and examined in a scanning electron microscope (Philips SEM 515).

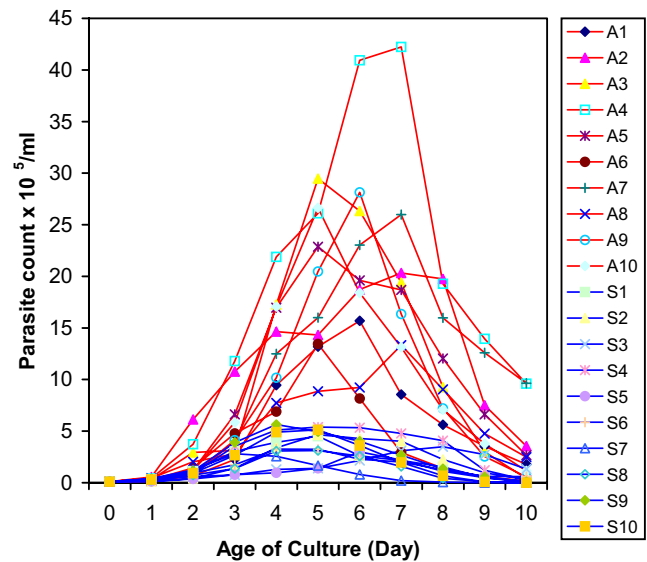


**Fig. 1** Growth profiles of asymptomatic (A1–A10) and symptomatic (S1–S10) isolates of *B. hominis* in Jones' medium containing 10% horse serum and incubated at 37°C. Asymptomatic isolates grew more rapidly than symptomatic isolates. Note: S7 died on day 9 while S8 and S10 died on day 10

#### Fluorescent lectin labeling of surfaces of symptomatic and asymptomatic isolates

Six asymptomatic isolates (Isolates A1, A3, A4, A5, A6 and A7) and six symptomatic isolates (Isolates S1, S3, S4, S5, S8 and S10) were randomly selected for surface carbohydrate analysis. Parasites were cultivated in Jones' medium as previously described. The parasites of the day-5 cultures of each isolate (peak parasite count, see Fig. 1) were harvested and subjected to fluorescein isothiocyanate (FITC)-lectin assays using three different lectins (Sigma, USA): *Canavalia ensiformis* (FITC-ConA), *Helix pomatia* (FITC-HPA) and *Triticum vulgare* (FITC-WGA).

FITC-labelled lectins were reconstituted in phosphate-buffered saline (PBS) pH 7.4 and dispensed in a total volume of 50 µl in 1.5-ml microtubes (Eppendorf, Germany). Parasite sediments from day 5 cultures were washed twice ( $500 \times g$ , 10 min) with PBS and diluted to a concentration of  $2 \times 10^7$  cells/ml. *B. hominis* cells were added to each FITC-lectin solution to a final volume of 100 µl. The mixture was incubated for 30 min at 37°C and subsequently centrifuged and washed twice ( $500 \times g$ , 10 min) with PBS. The pellets were reconstituted in 50 µl of PBS and 10 µl aliquots were examined by epifluorescence microscopy (Leitz, Wetzlar, Germany) at  $\times 400$  magnification. All experiments were performed in duplicate. The results of the FITC-lectin assays were quantitated with regard to: (1) percentage of fluorescent cells in 100 cells; (2) visual intensity of fluorescence (scale of brightness 0, 1+, 2+, 3+).

Subtyping *B. hominis* isolates

All 20 *B. hominis* isolates were subjected to sequenced-tagged site (STS) primer-polymerase chain reaction (PCR) using the seven sets of primers previously described by Yoshikawa et al. (2004). Parasites grown in Jones' medium were harvested by centrifugation (500×g, 5 min) and washed six times with sterile PBS. Pellets were lysed in lysis buffer (20 mM Tris-HCl buffer, pH 8.0, 100 mM NaCl, 25 mM ethylenediaminetetraacetic acid (EDTA), pH 8.0) containing 1% sodium dodecyl sulfate (SDS) and 0.5 mg proteinase K per milliliter (Fermentas, USA) and incubated at 55°C overnight. Genomic DNA was extracted with phenol/chloroform/isoamyl alcohol. Nucleic acids were precipitated with 0.3 M sodium acetate, pH 5.2 (final concentration) and two volumes of ice-cold ethanol. Following washing in 70% ice-cold ethanol, the DNA pellet was resuspended in 20–50 µl Tris-EDTA (TE) buffer containing 10 mM Tris and 1 mM EDTA, pH 8.0.

Two to five microliters of DNA preparations were used to amplify the genomic sequences in a 25-µl reaction containing 0.2 mM of the four deoxyribonucleotide triphosphates, 25 pmol of each primer, 1× PCR buffer (75 mM Tris-HCl, pH 8.8, 20 mM (NH<sub>4</sub>)<sub>2</sub>SO<sub>4</sub> and 0.01% Tween 20), 2.5 mM MgCl<sub>2</sub> and 1 U Taq DNA polymerase (recombinant) (Fermentas, USA). PCR conditions consisted of one cycle of initial denaturing at 94°C for 3 min, followed by 30 cycles including denaturing at 94°C for 30 s, annealing at 57°C for 30 s and extension at 72°C for 1 min and an additional cycle with a 10-min chain elongation at 72°C (thermocycler Eppendorf, Germany). The amplified products were electrophoresed in 1.5% agarose gels (Promega, USA) in Tris-borate-EDTA buffer. Gels were stained with ethidium bromide and photographed using an ultraviolet gel documentation system (Uvitec, United Kingdom). PCR amplification for each primer pair was repeated three times for each isolate.

## Results

### Growth characteristics

Over a 10-day period of cultivation in Jones' medium supplemented with 10% horse serum, asymptomatic isolates (A1–A10) showed higher growth rates than symptomatic isolates (S1–S10) (Fig. 1). Parasite counts for asymptomatic isolates peaked on day 5 for A3, A5, A6 and A10; day 6 for A1 and A9; and day 7 for A2, A4, A7 and A8. From initial parasite counts of  $1 \times 10^4$  cells/ml, peak counts for asymptomatic isolates ranged from  $1.33 \times 10^6$  cells/ml for A8 to  $4.22 \times 10^6$  cells/ml for A4 (Fig. 1). Most symptomatic isolates reached maximum parasite counts on

day 5 (S1, S2, S4, S8 and S10) and the peak parasite counts ranged from  $2.82 \times 10^5$  cells/ml (S7) to  $5.64 \times 10^5$  cells/ml (S9) (Fig. 1).

The generation time and number of generations per 24 h for all isolates are shown in Table 1. In the 20 isolates studied, the average generation time was  $12.3 \pm 4.3$  h and the number of generations per 24 h averaged  $2.2 \pm 0.7$ . Generally, asymptomatic isolates grew more rapidly (average generation time 9.3 h) than symptomatic isolates (average generation time 15.3 h). Isolate A2 showed the highest growth rate while S3 showed the slowest growth rate. At the period of maximum growth, asymptomatic isolates showed significantly lower generation time (higher growth rate) than symptomatic isolates ( $p < 0.05$ , Mann-Whitney test).

The size ranges of the various morphological forms of *Blastocystis* were as follows: vacuolar=5 to 90 µm; granular=10 to 35 µm and amoeboid=5 to 65 µm. Parasites from symptomatic isolates (S1–S10) were larger (mean=19.3–26.8 µm) with greater size variations (SD=8.3–14.2 µm) than parasites from asymptomatic isolates (A1–A10) (mean=12.6–20.0 µm; SD=3.8–6.6 µm). The

**Table 1** Generation time and number of generations per 24 h recorded for asymptomatic (A1–A10) and symptomatic (S1–S10) *B. hominis* isolates

Isolates	Period of maximum growth (days)	Generation time (h) <sup>a</sup>	Number of generations <sup>a</sup>
A1	3–4	11.7	2.1
A2	1–2	6.9	3.5
A3	1–2	7.5	3.2
A4	1–2	7.8	3.1
A5	1–2	8.4	2.9
A6	1–2	9.8	2.5
A7	1–2	9.4	2.6
A8	1–2	11.1	2.2
A9	2–3	10.8	2.2
A10	1–2	9.5	2.5
Mean ± SD		9.3±1.6	2.7±0.5
S1	1–2	14.7	1.6
S2	1–2	13.0	1.8
S3	1–2	26.7	0.9
S4	2–3	12.3	2.0
S5	1–2	14.7	1.6
S6	1–2	13.1	1.8
S7	1–2	14.6	1.6
S8	1–2	15.7	1.5
S9	2–3	13.5	1.8
S10	2–3	14.8	1.6
Mean ± SD		15.3±4.1	1.6±0.3

<sup>a</sup> The generation time and number of generations were determined for the 24-h period during which the most rapid growth occurred (see Fig. 1).

SD standard deviation.

median value for size also varied between each isolate. The median value of the symptomatic (S1–S10) isolates ranged from 17.5 to 25.0  $\mu\text{m}$ , but the asymptomatic isolates (A1–A10) exhibited smaller values of 12.5 to 20.0  $\mu\text{m}$ . Isolate S3 had the largest mean size (26.8  $\mu\text{m}$ ), while A5 had the smallest (12.6  $\mu\text{m}$ ). Some overlap in size was observed between symptomatic and asymptomatic isolates. Symptomatic isolates showed a significantly greater size range (42.5 to 85  $\mu\text{m}$ ) than asymptomatic isolates (17.5 to 30  $\mu\text{m}$ ) ( $p < 0.05$ , Mann–Whitney test; Fig. 2). The maximum size was noted in S10 (85  $\mu\text{m}$ ) and the minimum in A2 (17.5  $\mu\text{m}$ ).

#### Scanning electron microscopy

Asymptomatic isolates (A1, A3 and A4) generally appeared spherical and possessed a smooth surface with tiny pores (Fig. 3a,b). In contrast, two populations of parasites were observed in symptomatic isolates (S1, S8 and S10), namely, (1) spherical parasites with a rough, highly convoluted surface (Fig. 4a,b), and (2) irregularly shaped (amoeboid) parasites with large pseudopodia, projections and deep indentations. The surface of amoeboid forms appeared fibrillar in nature. The surface coat of symptomatic isolates, particularly amoeboid forms, appeared to be more frequently associated with bacteria (data not shown).

#### Surface coat carbohydrate reactivity

Symptomatic isolates consistently fluoresced more intensely (2+ to 3+) with FITC-ConA and FITC-HPA than asymptomatic isolates (1+) (Table 2). FITC-HPA fluorescence was more intense than FITC-ConA and FITC-WGA. FITC-WGA did not bind to A1, A3, A4, A7, S1 and S10. Isolates S4, S5 and S8 were agglutinated by FITC-HPA (Fig. 5).

#### Subtyping *B. hominis* isolates

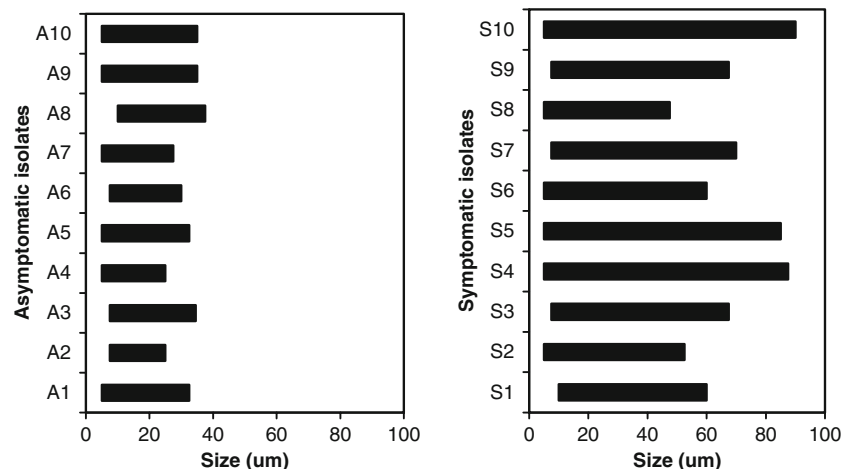
Using sequenced-tagged site primer-PCR, distinct PCR products of the expected sizes were produced for each particular subtype. Only subtypes 1, 2 and 3 were encountered in the present study (Fig. 6). All symptomatic isolates belonged to subtype 3 and all asymptomatic isolates were subtype 1, except A8, which was subtype 2.

#### Discussion

The recent surge of interest in *B. hominis* biology has been driven by the unresolved controversy concerning its role in pathogenicity. Several studies have attempted to differentiate symptomatic and asymptomatic isolates of *B. hominis* based on phenotypic characteristics such as isoenzyme patterns (Mansour et al. 1995; Gericke et al. 1997), serogroups (Müller 1994) and protein profiles (Kukoschke and Müller 1991; Lanuza et al. 1999) or genotypic characteristics such as molecular profiles and subtype signatures (Böhm-Gloning et al. 1997; Kaneda et al. 2001; Yoshikawa et al. 2004; Yan et al. 2006; Stensvold et al. 2007a,b,c). As yet, the use of both phenotypic and genotypic approaches to determining pathogenicity of the isolates studied has not been reported. The present study represents the first comparative study of both phenotypic and genotypic characteristics of asymptomatic and symptomatic human-derived *B. hominis* isolates.

In vitro culture of *Blastocystis* provides sufficient organisms for assessing phenotypic differences between isolates but has been subject to criticism in that it might preferentially amplify specific *Blastocystis* subtypes. Parkar et al. (2007) stated that in vitro culture of stool samples prior to PCR favored the preferential amplification of *Blastocystis* subtype 5 over subtype 1; however, Stensvold et al. (2007a) compared data obtained from DNA ex-

**Fig. 2** Comparison of size range between asymptomatic (A1–A10) and symptomatic (S1–S10) *B. hominis* isolates. Symptomatic isolates have a significantly greater size range than the asymptomatic isolates ( $p < 0.05$ , Mann–Whitney test)



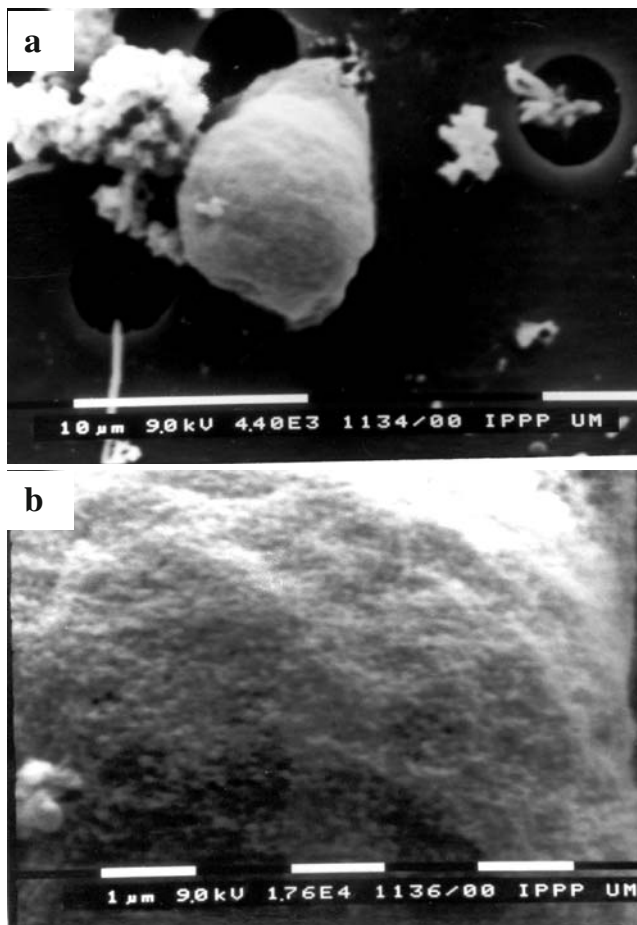


**Fig. 3** Scanning electron micrographs of an asymptomatic isolate of *B. hominis* grown in vitro. **a** Vacuolar form (A3) is covered by a surface coat. **b** Higher magnification of **a** showing a smooth surface with tiny pores

tracted directly from faeces and DNA extracted from 5- and 28-day-old in vitro cultures of ten randomly chosen *Blastocystis* isolates and demonstrated no differences, indicating that in vitro culture had little or no impact on subtype distribution or variation within a given specimen. Given the limited data available, the fact that in vitro culture had little or no impact on subtype distribution or variation over time led us to the conclusion that in vitro culture was a suitable method to use for this study.

As most growth profile studies and morphological analyses of *B. hominis* have been performed on small sample sizes and mostly on either symptomatic or asymptomatic isolates, or isolates without clinical histories, the relationships between *B. hominis* in vitro growth characteristics and morphology and its pathogenic potential, as determined by clinical and molecular subtyping criteria, have not been examined.

In the present study, two different groups of *B. hominis* isolates that could be differentiated in terms of their

morphology were identified. Asymptomatic isolates had a smaller size range, a greater abundance of granular forms and multiplied more rapidly in Jones' medium. In contrast, all symptomatic isolates exhibited a greater size range, the presence of amoeboid forms and multiplied more slowly in Jones' medium. This study also confirms the existence of the amoeboid *B. hominis* forms, which could be an indicator of the pathogenicity of the parasite, as stated in our previous study (Tan and Suresh 2006a). The present study indicates the potential usefulness of morphology as an inexpensive tool for identifying potentially pathogenic isolates of *B. hominis*, particularly following in vitro culture.

In in vitro culture, asymptomatic isolates (A1–A10) grew faster and achieved parasite counts approximately seven times greater than symptomatic isolates (S1–S10) at the period of peak growth. The average generation time for asymptomatic isolates was  $9.3 \pm 1.6$  h (range 6.9–11.7 h), but the average generation time for symptomatic isolates

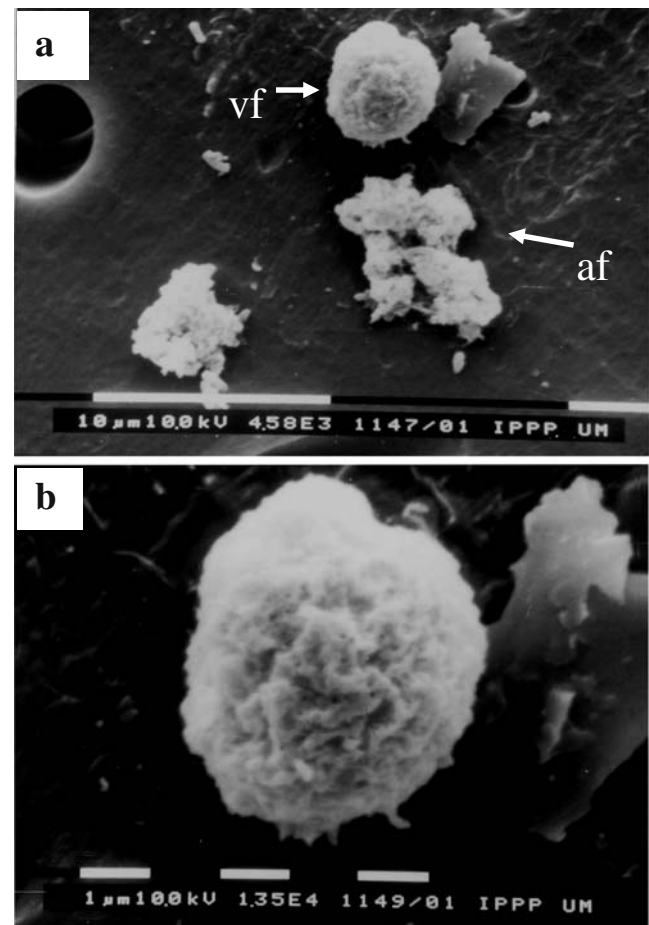


**Fig. 4** Scanning electron micrographs of symptomatic *B. hominis* isolate (S1) grown in vitro. **a** Two types of parasite cells can be seen: (1) a spherical vacuolar form (vf) and (2) an irregularly shaped, amoeboid form (af) with a rough surface and projections. **b** Higher magnification of **a** showing a vacuolar form with a rough surface

**Table 2** Intensity of fluorescence and percentage of fluorescent forms of *B. hominis* labelled with FITC-labelled lectins

Isolates	Fluorescence intensity (% fluorescent forms)					
	FITC-ConA (2 mg/ml)		FITC-HPA (1 mg/ml)		FITC-WGA (2 mg/ml)	
	Tube 1 <sup>a</sup>	Tube 2	Tube 1 <sup>a</sup>	Tube 2	Tube 1 <sup>a</sup>	Tube 2
<b>Asymptomatic isolates</b>						
A1	1+ (89)	1+ (95)	1+ (30)	1+ (56)	0 (0)	0 (0)
A3	1+ (100)	1+ (100)	1+ (40)	1+ (68)	0 (0)	0 (0)
A4	1+ (100)	2+ (90)	1+ (64)	1+ (85)	0 (0)	0 (0)
A5	1+ (100)	1+ (96)	1+ (55)	1+ (35)	1+ (35)	1+ (46)
A6	1+ (98)	1+ (100)	1+ (80)	1+ (76)	1+ (26)	1+ (45)
A7	1+ (100)	1+ (97)	1+ (74)	1+ (85)	0 (0)	0 (0)
<b>Symptomatic isolates</b>						
S1	2+ (100)	3+ (100)	3+ (98)	3+ (100)	0 (0)	0 (0)
S3	3+ (97)	3+ (95)	3+ (95)	3+ (100)	1+ (65)	1+ (54)
S4	3+ (100)	2+ (100)	3+ (100) <sup>b</sup>	3+ (100) <sup>b</sup>	1+ (68)	1+ (60)
S5	3+ (100)	3+ (95)	3+ (100) <sup>b</sup>	3+ (98) <sup>b</sup>	1+ (42)	1+ (53)
S8	3+ (95)	3+ (100)	3+ (100) <sup>b</sup>	3+ (100) <sup>b</sup>	1+ (74)	1+ (65)
S10	2+ (100)	3+ (98)	3+ (100)	3+ (97)	0 (0)	0 (0)

<sup>a</sup> All experiments performed in duplicate

<sup>b</sup> Agglutinated parasites observed.

was almost twice as long ( $15.3 \pm 4.1$  h, range 12.3–26.7 h) (Table 1). Thus, asymptomatic isolates multiplied at about twice the rate of symptomatic isolates. The reason for this remains unclear at present, but asymptomatic and symptomatic isolates may undergo different modes of reproduction in vitro. If the slower growth rate of symptomatic isolates in vitro give rise to low numbers of parasites in vivo, parasites may be less easily detected in stool samples, particularly if diagnosis is dependent on microscopic examination alone.

Previously, we described the surface morphology of the amoeboid form of *B. hominis* (Tan and Suresh 2006b). In

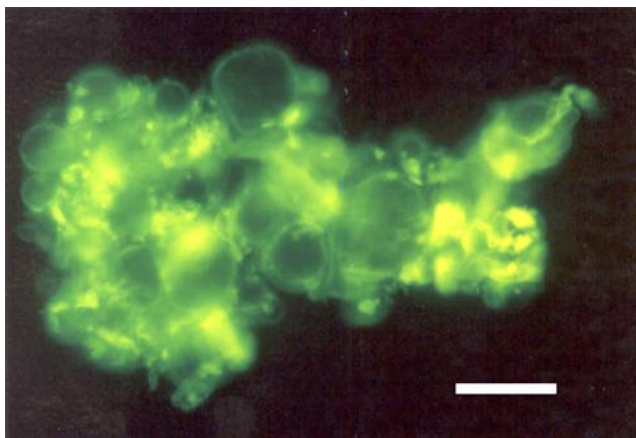


**Fig. 5** Epifluorescence images of FITC-labelled lectin binding *B. hominis* assays. A cluster of agglutinated cells showing fluorescence at the peripheral margin and in the central vacuole using FITC-HPA. Scale bar=20  $\mu$ m

the present study, we observed that vacuolar forms in symptomatic isolates showed a rougher surface than that seen in asymptomatic isolates. Bacteria were seen to adhere more frequently to the rougher surfaces of symptomatic isolates (data not shown), suggesting a close association between the surface coat and adherent bacteria. The major immune response in *Blastocystis*-infected patients is probably against surface coat carbohydrate (Tan et al. 2002), and humans react to the presence of the surface coat by producing an IgG<sub>2</sub> response, which is significantly stronger

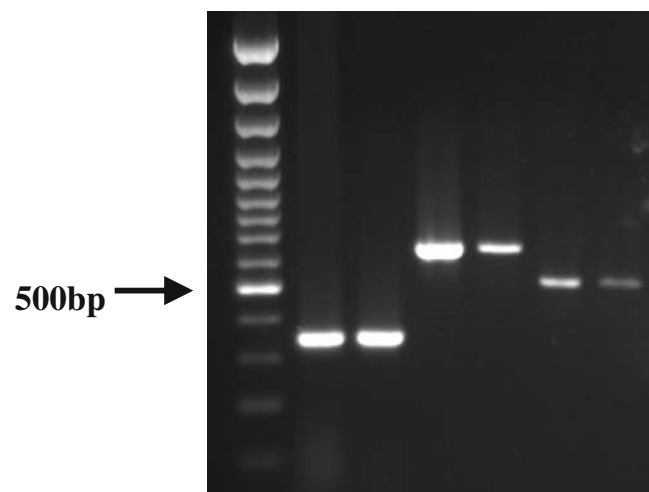


**Fig. 6** Examples of PCR products from *B. hominis* DNA amplified by sequenced-tagged site (STS) primers. Lane 1=DNA size markers of a 100-bp DNA ladder plus (Fermentas, USA); lanes 2 and 3= subtype 1 (351 bp); lanes 4 and 5= subtype 2 (650 bp); lanes 6 and 7= subtype 3 (526 bp)

in patients with irritable bowel syndrome as compared with normal individuals (Hussain et al. 1997).

Several studies have examined the surface morphology of *B. hominis* by SEM (Dunn et al. 1989; Boreham and Stenzel 1993; Suresh et al. 1994; Cassidy et al. 1994; Zaman et al. 1999). The smooth and pitted surface structure of *B. hominis* in asymptomatic isolates is similar to that described previously by Suresh et al. (1994). The rougher surface topography of the symptomatic isolates seen in the present study is comparable to the surface morphology of the isolate netsky of *B. hominis* (Boreham and Stenzel 1993), which was isolated from a patient suffering from diarrhoea in which *B. hominis* was the only parasite seen during thorough stool examination (Zierdt and Williams 1974). Hence, the observations in the present study add further weight to the possible relationship between surface morphology and the pathogenic potential of *B. hominis*; however, its significance remains to be elucidated.

Lanuza et al. (1996) examined 20 symptomatic *B. hominis* isolates and described strong binding affinities between both ConA and HPA and parasite outer surfaces. ConA exhibits specificity for a-D-mannosyl and a-D-glucosyl non-reducing terminal groups, HPA specifically binds *N*-acetyl-a-D-glucosamine and WGA binds *N*-acetyl- $\beta$ -D-glucosamine (Lanuza et al. 1996). In this study, parasites from symptomatic isolates consistently showed more intense surface fluorescence with both FITC-ConA and FITC-HPA than those from asymptomatic isolates (Table 2). Thus, our data for symptomatic isolates are in agreement with those of Lanuza et al. (1996). The presence of *N*-acetyl- $\beta$ -D-glucosamine (detected by WGA) was indicated in six (50%) of our isolates.

This suggests that the surface coat of parasites from our symptomatic isolates had higher surface accessible levels of a-D-mannosyl, a-D-glucosyl non-reducing terminal groups and *N*-acetyl- $\beta$ -D-glucosamine. We also noted differences in fluorescent lectin binding between and within asymptomatic and symptomatic isolates. Importantly, this is the first study to identify differences between symptomatic and asymptomatic isolates in terms of ConA and HPA binding, suggesting the potential usefulness of both ConA and HPA in assisting the differentiation of symptomatic and asymptomatic isolates.

Lectin-based studies have been used previously to identify surface-exposed carbohydrates associated with pathogenicity. Differences in surface properties were shown between *Entamoeba histolytica* isolated from carriers and those obtained from individuals with invasive amoebiasis (Martínez-Palomo et al. 1973; Trissl et al. 1977). Pathogenic strains of *E. histolytica* were agglutinated more easily with ConA than isolates from human asymptomatics (Trissl et al. 1977). Virulent strains of *E. histolytica* produce an abundance of lipophosphoglycan (LPG) and lipophospho-

peptidoglycan (LPPG), while avirulent *E. histolytica* and *E. dispar* produce either very low or no detectable levels of LPG, and either low levels or modified forms of LPPG on their cell surfaces (Moody et al. 1997). In *Acanthamoeba* keratitis, lectin-mediated adhesion to host cells is a prerequisite for amoeba-induced cytolysis of target cells (Cao et al. 1998).

Sugar inhibition assays revealed that *Acanthamoeba* lectin has the highest affinity for  $\alpha$ -Man and Man( $\alpha$ 1–3) Man units and in vitro cytopathic assays indicated that mannose-based saccharides, which inhibited amoeba adhesion to corneal epithelial cells, were also potent inhibitors of amoeba-induced cytopathic effect (Cao et al. 1998). Perhaps, as for *Acanthamoeba*, the adhesion of *B. hominis* to enterocytes is also carbohydrate-mediated. The higher level of a-D-mannosyl, a-D-glucosyl non-reducing terminal groups and *N*-acetyl- $\beta$ -D-glucosamine in parasites from symptomatic isolates, particularly in amoeboid forms, may facilitate the adhesion of these parasites to enterocytes, resulting in gastrointestinal illness. This hypothesis remains to be elucidated further.

Our previous phylogenetic analyses, based on arbitrarily primed polymerase chain reaction fingerprinting, using the same isolates (Tan et al. 2006) indicated that all symptomatic isolates (S1–S8) formed a clade with >70% similarity among the isolates and which were clearly separated from asymptomatic isolates A1, A3, A4, A5, A6 and A7. Asymptomatic isolate A8 formed a distinct clade. The results of our sequenced-tagged site primer-PCR subtype analysis of these isolates further support these findings. All symptomatic isolates (S1–S8) belonged to the same subtype (subtype 3), while all asymptomatic isolates, except A8, belonged to subtype 1. Isolate A8 belonged to subtype 2.

Yoshikawa et al. (2004) compared isolates from 15 symptomatic and 11 asymptomatic patients in Bangladesh using PCR-based subtype classification and found subtypes 1 and 3 in both symptomatic and asymptomatic cases, indicating a lack of correlation between specific subtypes and the pathogenic potential of *B. hominis*. Nevertheless, results from the present study indicate that subtype 3 correlated with disease, as all symptomatic isolates were subtype 3. This result contradicts the report by Yan et al. (2006) who suggested a possible relationship between subtype 1 and pathogenic potential, although they also found subtype 3 in symptomatic patients. More recently, Katsarou-Katsari et al. (2008) concurred with our findings in that a patient infected with *Blastocystis* sp. subtype 3 presented with acute urticaria and gastrointestinal symptoms. The particular *B. hominis* isolate was found to produce throughout in vitro cultivation.

The small-subunit (SSU) ribosomal RNA (rRNA) sequence divergence between ribodeme 2 (subtype 3) and ribodeme 1 (subtype 1) is over 7% (Clark 1997), which is

approximately four times the genetic distance between the homologous genes of the pathogen *E. histolytica* and the commensal *E. dispar* (Novati et al. 1996). This may help explain the remarkable phenotypic differences between asymptomatic and symptomatic isolates in the present study.

Since *B. hominis* subtype 3 has been previously reported from asymptomatic individuals (Yoshikawa et al. 2004; Yan et al. 2006; Stensvold et al. 2007a), current subtyping protocols may prove insufficient to determine the pathogenic potential of this parasite. Additional phenotypic evidence including the greater size range, the slower growth rate, the presence of the amoeboid form in in vitro culture, the strong surface fluorescence of FITC-HPA and FITC-ConA to in vitro forms and possibly HPA agglutination, which occurred only in our symptomatic isolates could assist current genotyping methods in determining the pathogenic potential of *B. hominis*.

Molecular phylogenies of *Blastocystis* from different hosts based upon the small-subunit (SSU) rRNA and elongation factor 1 $\alpha$  (EF-1 $\alpha$ ) gene sequences have led to the suggestion that more than one *Blastocystis* species can infect humans (Noël et al. 2005). Based on the phenotypic and genotypic differences between the asymptomatic and symptomatic isolates, we identify further phenotypic tools that should assist in determining the pathogenicity of *Blastocystis*.

## References

- Böhm-Gloning B, Knobloch J, Walderich B (1997) Five subgroups of *Blastocystis hominis* isolates from symptomatic and asymptomatic patients revealed by restriction site analysis of PCR amplified 16S-like rDNA. *Trop Med Int Health* 2:771–778
- Boreham PFL, Stenzel DJ (1993) *Blastocystis* in humans and animals: morphology, biology, and epizootiology. *Adv Parasitol* 32:1–70
- Cao Z, Jefferson DM, Panjwani N (1998) Role of carbohydrate-mediated adherence in cytopathogenic mechanisms of *Acanthamoeba*. *J Biol Chem* 273:15838–15845
- Cassidy MF, Stenzel DJ, Boreham PFL (1994) Electron microscopy of surface structures of *Blastocystis* sp. from different hosts. *Parasitology* 80:505–511
- Clark CG (1997) Extensive genetic diversity in *Blastocystis hominis*. *Mol Biochem Parasitol* 87:79–83
- Dunn LA, Boreham PFL, Stenzel DJ (1989) Ultrastructural variation of *Blastocystis hominis* stocks in culture. *Int J Parasitol* 19:43–56
- Fauque P, Ben Amor A, Joanne C, Agnani G, Bresson JL, Roux C (2007) Use of trypan blue staining to assess the quality of ovarian cryopreservation. *Fertil Steril* 87:1200–1207
- Gericke A, Burchard G, Knobloch J, Walderich B (1997) Isoenzyme patterns of *Blastocystis hominis* patient isolates derived from symptomatic and healthy carriers. *Trop Med Int Health* 2:245–253
- Hussain R, Jaferi W, Zuberi S, Baqai R, Abrar W, Ahmed A, Zaman V (1997) Significantly increased IgG2 subclass antibody levels to *Blastocystis hominis* in patients with irritable bowel syndrome. *Am J Trop Med Hyg* 56:301–305
- Jones WR (1946) The experimental infection of rats with *Entamoeba histolytica* with a method for evaluating the anti-amoebic properties of new compounds. *Ann Trop Med Parasitol* 40:130–140
- Kaneda Y, Horiki N, Cheng XJ, Fujita Y, Maruyama M, Tachibana H (2001) Ribodemes of *Blastocystis hominis* isolated in Japan. *Am J Trop Med Hyg* 65:393–396
- Katsarou-Katsari A, Vassalos CM, Tzanetou K, Spanakos G, Papadopoulou C, Vakalis N (2008) Acute urticaria associated with amoeboid forms of *Blastocystis* sp. subtype 3. *Acta Derm Venereol* 88:80–81
- Kukoschke KG, Müller HE (1991) SDS-PAGE and immunological analysis of different axenic *Blastocystis hominis* strains. *J Med Microbiol* 35:35–39
- Lanuza MD, Carbajal JA, Borrás R (1996) Identification of surface coat carbohydrates in *Blastocystis hominis* by lectin probes. *Int J Parasitol* 26:527–532
- Lanuza MD, Carbajal JA, Villar J, Mir A, Borrás R (1999) Soluble protein and antigenic heterogeneity in axenic *Blastocystis hominis* isolates: pathogenic implications. *Parasitol Res* 85:93–97
- Mansour NS, Mikhail EM, El Masry NA, Sabry AG, Mohareb EW (1995) Biochemical characterisation of human isolates of *Blastocystis hominis*. *J Med Microbiol* 42:304–307
- Martínez-Palomo A, González-Robles A, de la Torre M (1973) Selective agglutination of pathogenic strains of *Entamoeba histolytica* induced by concanavalin A. *Nature New Biol* 245:186–188
- Moody S, Becker S, Nuchamowitz Y, Mirelman D (1997) Virulent and avirulent *Entamoeba histolytica* and *Entamoeba dispar* differ in their cell surface phosphorylated glycolipids. *Parasitology* 114:95–104
- Müller H (1994) Four serologically different groups within the species *Blastocystis hominis*. *Zentralbl Bakteriol* 280:403–408
- Noël C, Dufernez F, Gerbod D, Edgcomb VP, Delgado-Viscogliosi P, Ho LC, Singh M, Wintjens R, Sogin ML, Capron M, Pierce R, Zenner L, Viscogliosi E (2005) Molecular phylogenies of *Blastocystis* isolates from different hosts: Implications for genetic diversity, identification of species, and zoonosis. *J Clin Microbiol* 43:348–355
- Novati S, Sironi M, Granata S, Bruno A, Gatti S, Scaglia M, Bandi C (1996) Direct sequencing of the PCR amplified SSU rRNA gene of *Entamoeba dispar* and the design of primers for rapid differentiation from *Entamoeba histolytica*. *Parasitology* 112:363–369
- Parkar U, Traub RJ, Kumar S, Munghthin M, Vitali S, Leelayoova S, Morris K, Thompson RC (2007) Direct characterization of *Blastocystis* from faeces by PCR and evidence of zoonotic potential. *Parasitology* 134:359–367
- Stensvold CR, Arendrup MC, Jespersgaard C, Mølbak K, Nielsen HV (2007a) Detecting *Blastocystis* using parasitologic and DNA-based methods: a comparative study. *Diagn Microbiol Infect Dis* 59:303–307
- Stensvold CR, Traub RJ, von Samson-Himmelstjerna G, Jespersgaard C, Nielsen HV, Thompson RCA (2007b) *Blastocystis*: subtyping isolates using Pyrosequencing™ technology. *Exp Parasitol* 116:111–119
- Stensvold CR, Suresh GK, Tan KSW, Thompson RCA, Traub RJ, Viscogliosi E, Yoshikawa H, Clark CG (2007c) Terminology for *Blastocystis* subtypes—a consensus. *Trends Parasitol* 23:93–96
- Suresh K, Smith H (2004) Comparison of methods for detecting *Blastocystis hominis*. *Eur J Clin Microbiol Infect Dis* 23:509–511
- Suresh K, Howe J, Ng GC, Ho LC, Ramachandran NP, Loh AK, Yap EH, Singh M (1994) A multiple fission-like mode of asexual reproduction in *Blastocystis hominis*. *Parasitol Res* 80:523–527
- Suresh K, Anuar K, Smith HV (2003) Multiple reproductive processes in *Blastocystis*. *Trends Parasitol* 18:528
- Tan KSW, Singh M, Yap EH (2002) Recent advances in *Blastocystis hominis* research: hot spot in terra incognita. *Int J Parasitol* 32:789–804

- Tan TC, Suresh KG (2006a) Predominance of amoeboid forms of *Blastocystis hominis* in isolates from symptomatic patients. *Parasitol Res* 98:189–193
- Tan TC, Suresh KG (2006b) Amoeboid form of *Blastocystis hominis*—a detailed ultrastructural insight. *Parasitol Res* 99:737–742
- Tan TC, Suresh KG, Thong KL, Smith HV (2006) PCR fingerprinting of *Blastocystis* isolated from symptomatic and asymptomatic human hosts. *Parasitol Res* 99:459–465
- Trissl D, Martínez-Palomo A, Arguello C, de la Torre M, de la Hoz R (1977) Surface properties related to concanavalin A-induced agglutination. A comparative study of several *Entamoeba* strains. *J Exp Med* 145:652–665
- Yan Y, Su S, Lai R, Liao H, Ye J, Li X, Luo X, Chen G (2006) Genetic variability of *Blastocystis hominis* isolates in China. *Parasitol Res* 99:597–601
- Yoshikawa H, Wu Z, Kimata I, Iseki M, Ali IK, Hossain MB, Zaman V, Haque R, Takahashi Y (2004) Polymerase chain reaction-based genotype classification among human *Blastocystis hominis* populations isolated from different countries. *Parasitol Res* 93:22–29
- Zaman V (1997) Phase-contrast microscopy of cell division in *Blastocystis hominis*. *Ann Trop Med Parasitol* 91:223–224
- Zaman V, Howe J, Ng M, Goh TK (1999) Scanning electron microscopy of the surface coat of *Blastocystis hominis*. *Parasitol Res* 85:974–976
- Zierdt CH, Williams RL (1974) *Blastocystis hominis*: axenic cultivation. *Exp Parasitol* 36:233–243
- Zierdt CH, Swan JC (1981) Generation time and growth rate of the human intestinal parasite *Blastocystis hominis*. *J Protozool* 28:483–485